WATER VAPOR ON MARS: A REFINED CLIMATOLOGY AND NEAR-SURFACE CONCENTRATION ENABLED BY SYNERGISTIC RETRIEVALS

E W. Knutsen, *LATMOS/IPSL, UVSQ Université Paris-Saclay, Sorbonne Université, CNRS, Guyancourt, France* (elise-wright.knutsen@latmos.ipsl.fr), **F. Montmessin**, *LATMOS/IPSL, UVSQ Université Paris-Saclay, Sorbonne Université, CNRS, Guyancourt, France*, **L. Verdier**, *LATMOS/IPSL, UVSQ Université Paris-Saclay, Sorbonne Université, CNRS, Guyancourt, France*, **G. Lacombe**, *LATMOS/IPSL, UVSQ Université Paris-Saclay, Sorbonne Université, CNRS, Guyancourt, France*, **F. Lefèvre**, *LATMOS/IPSL, UVSQ Université Paris-Saclay, Sorbonne Université, CNRS, Guyancourt, France*, **S. Ferron**, *ACRI-ST, boulevard des Garennes, Guyancourt, France*, **M. Giuranna**, *IAPS-INAF, Rome, Italy*, **P. Wolkenberg**, *IAPS-INAF, Rome, Italy*, **A. Fedorova**, *Space Research Institute (IKI), Moscow, Russia*, **A. Trokhimovskiy**, *Space Research Institute (IKI), Moscow, Russia*, **O. Korablev**, *Space Research Institute (IKI), Moscow, Russia.*

Introduction:

Until recently, knowledge of the near-surface H_2O profile on Mars mostly relied on general circulation models. The vertical distribution of water vapor has been inferred from nadir measurements (e.g.[1], [2]) and measured directly by solar occultation viewing geometry with SPICAM on Mars Express since 2004, and with the ExoMars Trace gas Orbiter and its infrared spectrometers NOMAD and ACS since 2018 (e.g. [3], [4]).

With solar occultation measurements, a very fine vertical resolution can be obtained, yet measurements below 10 km are sparse as aerosols at low altitudes lead to high opacities which significantly reduce the transmittance. The lower limit for observation is typically 5-10 km for dust-free conditions, and as high as 20-30 km during the dusty perihelion season (e.g., Aoki et al., [3]). Only under very clear conditions are solar occultation observations able to probe below 10 km, however such conditions mostly occur at high latitudes. As a result, information about the low-atmosphere water vapor profile remains exceptional.

Below 10 km, surface-atmosphere interactions such as convection, frost sublimation and deposition are expected to be the main forcers on the vertical distribution, along with adsorption and desorption. Above 10 km, water ice clouds are thought to be dominant [5], [6]. Below the saturation level, controversy exists regarding whether water vapor is well mixed with CO_2, or distributed in a more complex manner.

The goal of this study is two-part: firstly, to distinguish the near-surface water content from the rest of the column, and secondly, by having constrained the near-surface concentration, a refined and highly accurate water vapor climatology is obtained. The intention of this study is to be largely descriptive, as this is the first time the spectral synergy has been applied to a large dataset.

Method:

Two infrared spectrometers onboard the Mars Express satellite were utilized for this work. Water vapor column abundances were retrieved simultaneously with PFS (sensing the thermal infrared range) and SPICAM (sensing the near-infrared range), yielding distinct yet complementary sensitivity to different parts of the atmospheric column.

TIR measurements are mostly sensitive to the middle atmosphere (at the origin of the photon emission) where the temperature contrast of the atmosphere with respect to the surface is high. NIR measurements on the other hand are sensitive to any molecule present along the column as the technique relies on solar photons traversing the entire atmosphere back and forth.

When observing an atmosphere in nadir viewing geometry, the outcome is normally a column abundance value of the target species. However, it is possible to obtain information about the vertical distribution of the species by combining multiple spectral domains in the retrieval process.

By combining two spectral domains, the degree of freedom of the signal (DOF) is increased compared to single-domain retrievals. The DOF gives an estimate of the number of independent bits of information in an atmospheric measurement [7], and a DOF higher than 1 indicates the presence of some amount of profile shape information.

Dataset and retrieval. The synergistic approach requires a set of co-located PFS and SPICAM observations on which to apply the retrieval method. The dataset presented here consists of co-located observations taken over 1379 individual orbits distributed across seven Mars years from Ls 334° of MY 26 to Ls 297° of MY 34, with no measurements from MY 30-31.

To obtain a satisfying PFS SNR for the fitting of multiple parameters, nine consecutive spectra are averaged together. The SPICAM observation closest in time to the central PFS spectrum is then selected

and averaged with the seven observations prior to it and the seven after it, resulting in a combined FOV similar to that of the nine combined PFS observations.

A priori water vapor and temperature profiles are extracted from the Mars Climate Database (MCD) version 5.3, based on the general circulation model developed at the Laboratoire de Météorologie Dynamique (LMD GCM), [8], [9].

Temperature and aerosol parameters are retrieved individually from the PFS average spectra, which are then injected into the synergistic routine. The overall spectral fitting procedure uses the HITRAN 2012 spectroscopic database [10] as a baseline for the computation of absorption coefficients of H_2O and CO_2, and then relies on a Bayesian approach that consists in maximizing the probability that a given retrieval satisfies both the observed averaged spectra and falls within a range of plausible a priori values specified by assumptions on the value and its dispersion. The weight of the a priori assumption in the retrieval is dictated by its a priori uncertainty, which is set equal to the integrated a priori water vapor profile.

Water vapor is inferred from the set of combined NIR and TIR spectra, by a simultaneous inversion from both spectral domains. In practice, the algorithm adjusts the water vapor abundance along the vertical profile at nine altitude points separated by 2.5 km from ground to 10 km, and by 5 km from 10 to 30 km. All points are correlated with a Gaussian kernel, such that the points are less strongly correlated when the distance between them is increasing. Some example spectra are shown in the top row of Figure 1, where the selected NIR and TIR spectral intervals include strong diagnostic features of water vapor. The co-located observations shown here are from early summer of MY 27 at high latitudes. The corresponding vertical profile obtained from the synergistic retrieval is shown in the bottom left, and is compared to the MCD a priori profile. In the bottom right panel, the synergy is compared to the single spectral domain retrievals by computing ratios of a posteriori-to-a priori (post-to-prior for short) error profiles. MCD a priori profiles are used for all retrieval techniques (synergy, PFS-only, SPICAM-only). The post-to-prior profile indicates the amount of added information at each altitude, and shows that the synergy is more sensitive to the lower atmosphere than both PFS and SPICAM.

Results:

After imposing a series of selection criteria to ensure retrievals with satisfactory quality and sufficient vertical information to justify further analysis, a global composite climatology is assembled, as shown in Figure 2.

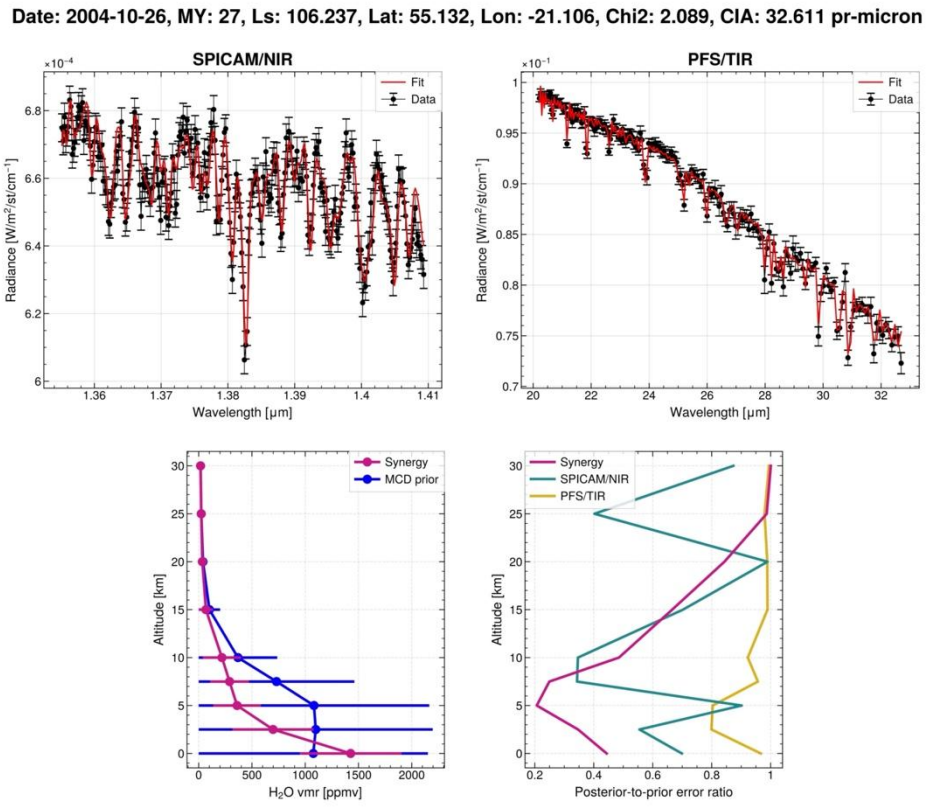

Figure 1: Example spectra from SPICAM and PFS, with the corresponding retrieved vertical profile and the a priori profile, along with the a posteriori-to-a priori ratios for the synergy and the single domain retrievals.

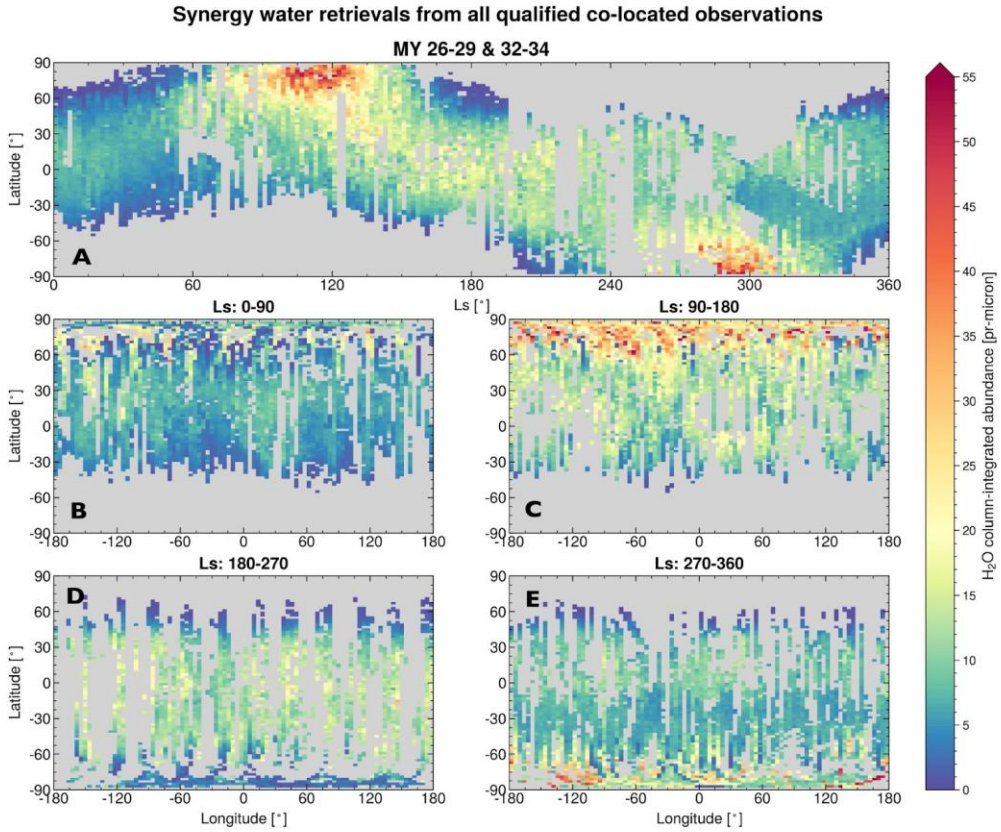

Figure 2: Seasonal and geographical variations in normalized total column abundances of water vapor. Panel A: Seasonal distribution of all qualified retrievals averaged in bins of 2°x2° Ls and latitude. Panels B-E: Geographical distribution of qualified retrievals for each seasonal interval, averaged in bins of 2°x4° latitude and longitude.

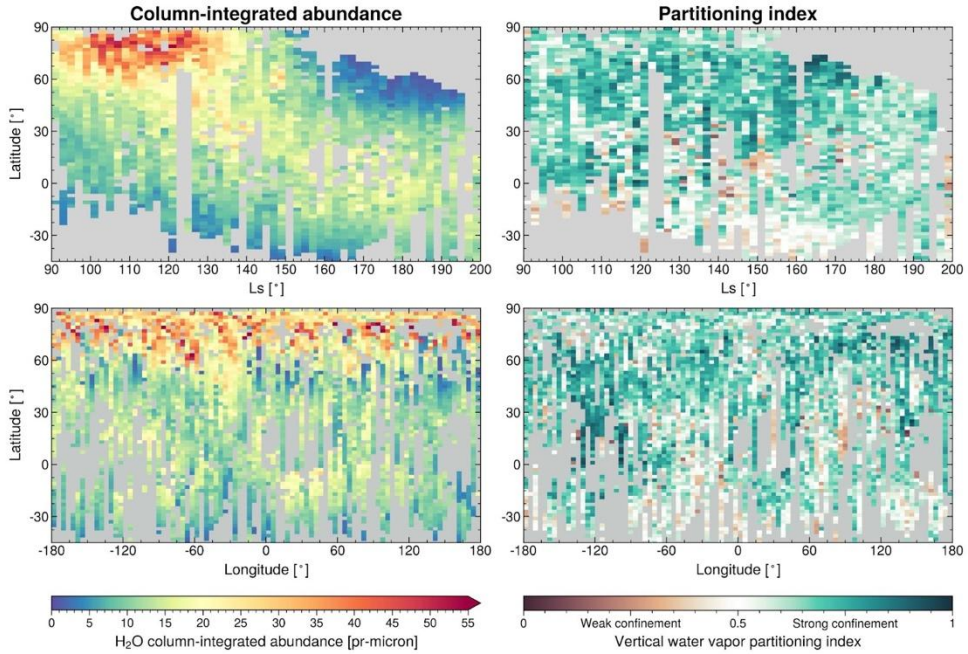

Figure 3: Composite maps of normalized water vapor column-integrated abundance and partitioning index. For the partitioning index, values higher than 0.5 (in green) indicate that more than 50% of the water vapor column is confined below 5 km, while lower values (in brown) indicate that water vapor is more evenly dispersed with altitude. Data from all available years fulfilling all requirements have been averaged in bins of 2° latitude, 2° Ls and 4° longitude.

Even with a DOF higher than with regular single-domain retrievals, the synergy still cannot resolve a vertical profile with several completely independent points. Because of this, we have defined a parameter called the Partitioning index (PI), a dimensionless value defined as the ratio of the column integrated water content from the surface up to 5 km, divided by the full column abundance. The PI is thus a measure of the near-surface water concentration, ranging from 0 (no water in the first 5 km) to 1 (all water contained below 5 km).

Figure 3 focuses on the Northern hemisphere spring and summer season, and shows the average trends in the total column abundance and PI at latitudes between 45°S and the North Pole, covering the polar ice sublimation season.

References:

[1] T. Fouchet *et al.*, "Martian water vapor: Mars Express PFS/LW observations," *Icarus*, vol. 190, no. 1, pp. 32–49, Sep. 2007, doi: 10.1016/j.icarus.2007.03.003.

[2] A. A. Pankine and L. K. Tamppari, "Constraints on water vapor vertical distribution at the Phoenix landing site during summer from MGS TES day and night observations," *Icarus*, vol. 252, pp. 107–120, May 2015, doi: 10.1016/j.icarus.2015.01.008.

[3] S. Aoki *et al.*, "Water Vapor Vertical Profiles on Mars in Dust Storms Observed by TGO/NOMAD," *J. Geophys. Res. Planets*, vol. 124, no. 12, pp. 3482–3497, Dec. 2019, doi: 10.1029/2019JE006109.

[4] A. Fedorova *et al.*, "Stormy water on Mars: The distribution and saturation of atmospheric water during the dusty season," *Science*, vol. 367, no. 6475, pp. 297–300, Jan. 2020, doi: 10.1126/science.aay9522.

[5] F. Montmessin, F. Forget, P. Rannou, M. Cabane, and R. M. Haberle, "Origin and role of water ice clouds in the Martian water cycle as inferred from a general circulation model," *J. Geophys. Res.*, vol. 109, no. E10, p. E10004, 2004, doi: 10.1029/2004JE002284.

[6] M. I. Richardson, "Investigation of the nature and stability of the Martian seasonal water cycle with a general circulation model," *J. Geophys. Res.*, vol. 107, no. E5, p. 5031, 2002, doi: 10.1029/2001JE001536.

[7] C. D. Rodgers, *Inverse Methods for Atmospheric Sounding: Theory and Practice*, vol. 2. WORLD SCIENTIFIC, 2000. doi: 10.1142/3171.

[8] F. Forget *et al.*, "Improved general circulation models of the Martian atmosphere from the surface to above 80 km," *J. Geophys. Res.*, vol. 104, no. E10, pp. 24155–24175, Oct. 1999, doi: 10.1029/1999JE001025.

[9] E. Millour, F. Forget, A. Spiga, M. Vals, V. Zakharov, and L. Montabone, "The Mars climate database (version 5.3)," *Paper presented at the Mars Science Workshop "From Mars Express to ExoMars", held 27-28 February 2018 at ESAC, Spain, id.68.*, Feb. 2018.

[10] L. S. Rothman *et al.*, "The HITRAN2012 molecular spectroscopic database," *Journal of Quantitative Spectroscopy and Radiative Transfer*, vol. 130, pp. 4–50, Nov. 2013, doi: 10.1016/j.jqsrt.2013.07.002.